24th INTERNATIONAL CONGRESS ON SOUND AND VIBRATION
23–27 July 2017, London

FULL-FIELD MODAL IDENTIFICATION FROM EXPERIMENTAL TRANSMISSIBILITY FUNCTIONS

Ángel Molina-Viedma, Elías López-Alba and Francisco Díaz

Universidad de Jaén, Departamento de Ingeniería Mecánica y Minera, Campus Las Lagunillas, Jaén, Spain
email: ajmolina@ujaen.es

Base motion excitation tests are very common when experimental modal analyses are required in real aerospace structures. In these cases, base motion represents better than a force excitation the behaviour of the structure. For general modal characterisation, some techniques such as laser vibrometry have been employed and compared with traditional transducers. More recently, the technique 3D Digital Image Correlation has been employed for modal characterisations using High Speed cameras (HS 3D-DIC). The advantage of HS 3D-DIC over traditional transducers is that it is non-invasive and provides a full-field measurement. Hence, this technique is particularly interesting for mode shapes identification since it increases the spatial resolution. However, the amount of data that is managed involves long processing times. In this study, a methodology for modal parameter estimation based on HS 3D-DIC it is presented. Full-field transmissibility functions of a cantilever beam were determined. An accelerometer was used to experimentally validate HS 3D-DIC measurements. Modal parameter estimation was performed using the circle-fit method. This method makes a single degree of freedom assumption, reducing the processing computational costs. Since it is designed to deal with frequency response functions, a theoretical conversion of transmissibility functions to FRFs is also proposed. Results were validated by numerical and analytical models. Finally, the Modal Assurance Criterion (MAC) has been employed to compare the mode shapes.

Keywords: experimental modal analysis, Digital Image Correlation, damping ratios, high speed cameras, base motion excitation

1. Introduction

Experimental modal analysis is an important task in all the fields of industry for the identification of modal parameters and validation of numerical models [1]. Depending on the features of the studied element, there may be limitations on the use of invasive, pointwise transducers such as accelerometers. Digital Image Correlation (DIC) [2], which is consolidated in experimental mechanics, is a non-invasive full-field optical technique for displacement measuring that provides solutions to this limitations. Particularly, it offers greater spatial resolution measurement, improving identification especially for mode shapes, and eludes mass-loading effect, providing measurement of the real behaviour. When used with high speed cameras, DIC is presented as a promising technique for full-field experimental modal analysis.

In fact, some research performed different methodologies for modal identification using DIC and high speed cameras (HS 3D-DIC) [3]–[5]. Results were compared and validated with accelerometer and Scanning Laser Doppler Vibrometry measurements. Despite achieving good results, just relation between displacement response and force excitation were considered. However, base motion tests are a common tool for vibration testing and modal identification considering base motion excitation instead of force [6]. Ha et al. [7] considered this kind of excitation to explore HS 3D-DIC capabilities in an artificial beetle's wing. Despite transfer functions were used for natural frequencies and damping ratios identification, damping ratios were calculated using half power method from the smoothed

transmissibility functions. Moreover, mode shapes were obtained carrying out additional tests, forcing resonances with sinusoidal excitation.

According to this, full-field transmissibility functions were employed in this study in order to carry out a complete modal parameter identification, involving natural frequencies, mode shapes and damping ratios, by means of a unique random excitation test. A stepped cantilever bar, manufactured in 2024 aluminium, was the element of study (Figure 1). This bar is known as Reference Material (RM) and intended for optical sets calibration [8]. Vibration were induced in the thinner part of the stepped cantilever part whereas the thicker part is uses for clamping purposes. Modal identification were performed using circle-fit approach [1] available in EasyMod [9], a free toolbox for modal identification in Matlab. The approach is intended for dealing with Frequency Response Functions (FRFs), so a theoretical transformation from transmissibility functions to FRFs were carried out, making single degree of freedom assumptions.

Theoretical and Finite Element Method (FEM) models were evaluated so as to validate the experimental methodology. Furthermore, accelerometers were used for experimental validation purpose. Modal Assurance Criterion (MAC) [10] was considered in order to provide a quantitative indicator regarding mode shapes.

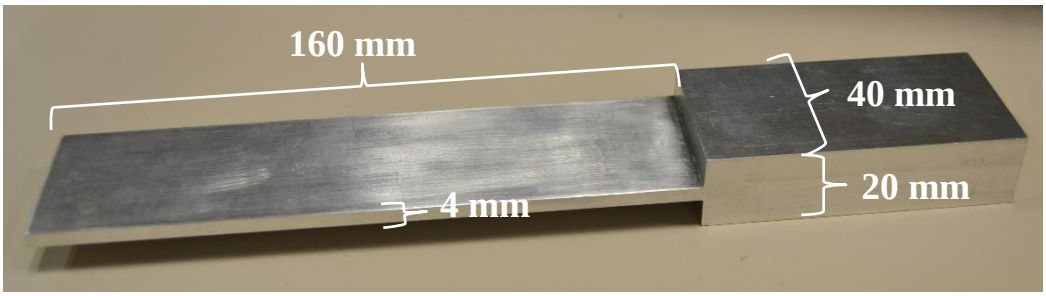

Figure 1: Reference Material

2. Experimental analysis

2.1 Experimental set-up

Experimental test was performed applying a flat random excitation up to 1000 Hz by means of an electrodynamic shaker. The thinner part of the Reference Material behaves as a cantilever beam when the thicker part is fixed to the shaker's armature what involves base motion excitation, as Figure 2 shows. In this spectrum, the first two bending modes of the cantilever were excited.

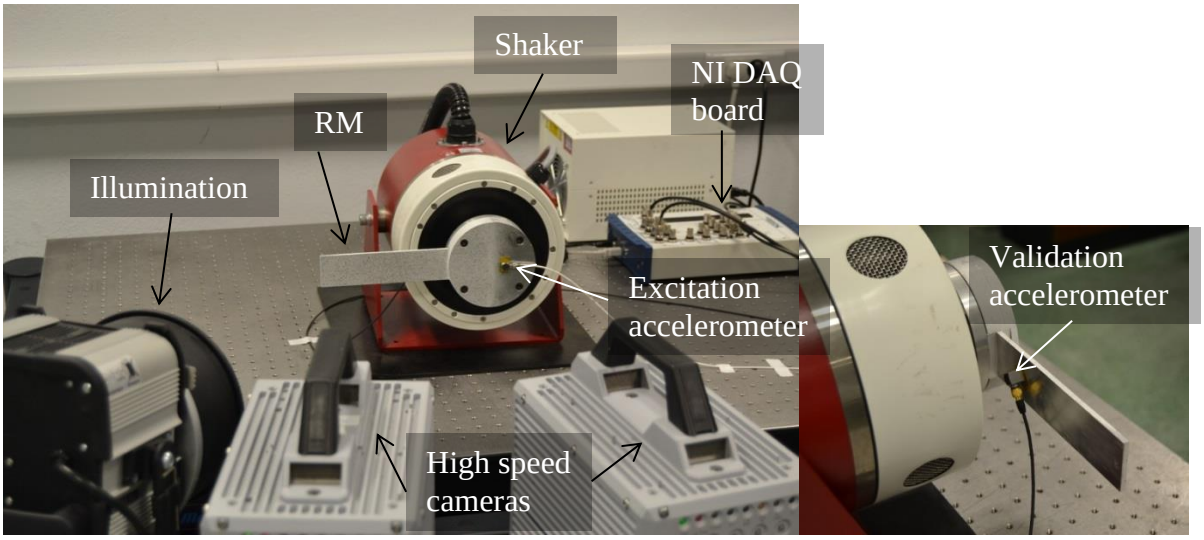

Figure 2: Experimental set up for modal analysis

Figure 2 also shows the optical equipment for DIC measurement. The main elements are two Fast-Cam SA4 (Photron) high speed cameras which recorded the RM during the test. Considering the maximum excitation frequency, 2000 frames per second were taken. Due to the short exposure time that high speed capture ratio involves, it was necessary to use a 150W lamp so as to achieve uniform light intensity. In order to obtain a transfer function between excitation and response, an accelerometer was attached to the clamping system. The DAQ system (NI USB-6251 DAQ) was used for registering accelerometer signal and synchronising with high speed cameras.

As previously said, experimental validation was required. Thus, an accelerometer was fixed to the rear surface of the beam, as seen in Figure 2, placed at 35 mm from the clamped edge of the beam. Close to the clamp, accelerometer's mass inertia is non-significant, reducing mass-loading effect. Transmissibility function from both accelerometer was also obtained.

2.2 Data processing

Mainly, processing tasks involves DIC analysis of the images from the tests, transmissibility functions calculation and modal identification algorithms execution.

DIC measurement is based on the identification and tracking of small regions in the area of interest of the specimen, known as facets. The surface must present a grey-scale random pattern, known as speckle (Figure 3), making every facet different from each other. The commercial Vic-3D software (Correlated Solutions) was employed to carry out DIC processing of the images. It resulted in a matrix of 66x246 measurement points along the beam's surface. At every point there is a time domain displacement vector. Along with accelerometer signal, frequency analysis of the vectors was performed so as to determine the transmissibility functions.

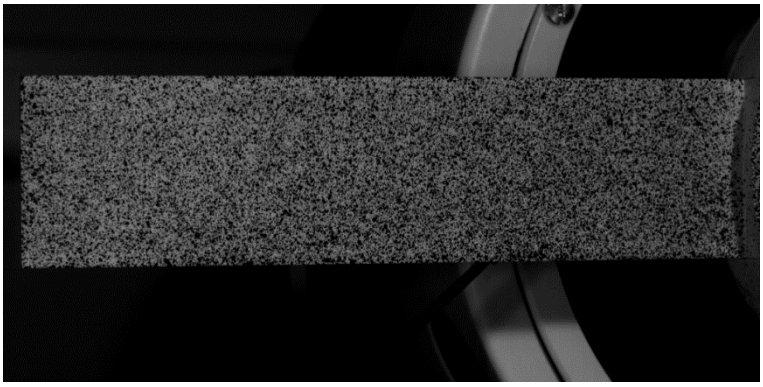

Figure 3: Speckle pattern for DIC measurement in the RM

Before modal identification, it was necessary to adapt transmissibility functions to circle-fit approach algorithm. As previously said, circle-fit method is intended for managing FRFs. Based on single degree of freedom assumptions, in this study a theoretical approach is proposed for obtaining equivalent FRFs from transmissibility functions. As circle-fit approach evaluates the vicinity of the resonance in FRF [1], if there is reasonable distance between resonances, it may be assumed that FRF and transmissibility function are defined by Eqs. (1)-(2) respectively:

$$H(i\omega) = \frac{1}{1-(\omega/\omega_n)^2 + i\eta} \tag{1}$$

$$T(i\omega) = \frac{(\omega/\omega_n)^2}{1-(\omega/\omega_n)^2 + i\eta} \tag{2}$$

Both equations represent the theoretical expression of a single degree of freedom system with structural damping, η, where ω_n represents the natural frequency [1]. It can be found out a relation between both functions as:

$$H(i\omega) = \frac{T(i\omega)}{(\omega/\omega_n)^2} \tag{3}$$

Thus, Eq. (3) represents the equivalent FRF of the experimental transmissibility function in the vicinity of each resonance individually. Circle-fit method could be then done for proper modal identification.

3. Theoretical analysis

Theoretical expression for the calculation of natural frequencies and mode shapes of a cantilever beam are respectively defined in Eqs. (4)-(5) [11]:

$$f_{n,i} = \frac{\beta_n^2}{2\pi}\sqrt{\frac{EI}{M}} \tag{4}$$

$$w_n(x) = (\sin \beta_n x - \sinh \beta_n x - \alpha_n(\cos \beta_n x - \cosh \beta_n x)) \tag{5}$$

They depend on specimen's properties like Young's Modulus, E, and mass, M, and the second moment of area, I. Additionally, there are two parameters, β_n and α_n, whose values for the first two bending modes are presented in Table 1. For comparison purposes, mode shapes from Eq. (5) were normalised to unity.

Table 1: Numerical parameters for analytical estimation of natural frequencies and mode shapes of the first two bending modes of a cantilever beam

N	β_n	α_n
1	11.719400	1.362221
2	29.338069	0.981868

4. Results

First results, consisted of a matrix of full-field transmissibility functions representing the whole surface of the beam, showed two resonance peak. In Fig. 4, experimental transmissibility functions from DIC and the validation accelerometer measurement are plotted corresponding to a point placed at 35 mm from the clamping (see Fig. 2). It can be seen the mentioned two bending modes as two corresponding peaks. Both functions are almost identical despite the higher level of noise presented in DIC. Considering that accelerometers are transducers with high sensitivity, DIC measurement is noisier because displacement gets lower as frequency increases, as well. Comparison of Power Spectral Density (PSD) at that point is shown in Fig. 5. It is observed that displacement at high frequency are lower than the noise floor of DIC (10^{-9} mm^2/Hz). That is the reason why transmissibility functions are not coincident in the interval from 850 Hz to 1000 Hz. An additional fact to be considered is that the point is close to the clamping, where the lowest displacement take place. However, anti-resonance event after the first mode is perfectly characterised by DIC despite being low level response.

Once identified the two peaks and determined the equivalent FRFs, circle-fit approach is required. The vicinity of each peak had to be defined. After evaluating different intervals, 132 Hz up to 137 Hz for the first mode and 760 Hz up to 777 Hz for the second one, were eventually determined considering the stability of fitting and consistency of the results throughout the beam. The results of the fitting can be analysed observing the Nyquist and Bode diagrams, shown in Fig. 6, corresponding to the second mode when fitting the FRF of a point at the released tip of the beam. Similar results were obtained from the first peak with less frequency lines in the analysed range.

As a result of this analysis, three matrices are provided corresponding to natural frequency, amplitude and damping ratio. So as to reduce the matrices to an only value, natural frequency and damping

ratio were obtained by calculating the mean value of the matrices. Hence, the first natural frequency was 135.38 Hz and the structural damping ratio of this mode was 1.69%, whereas for the second mode the natural frequency was 767.78 Hz with the damping ratio of 1.45%. The standard deviation was less than 1% in any case studied.

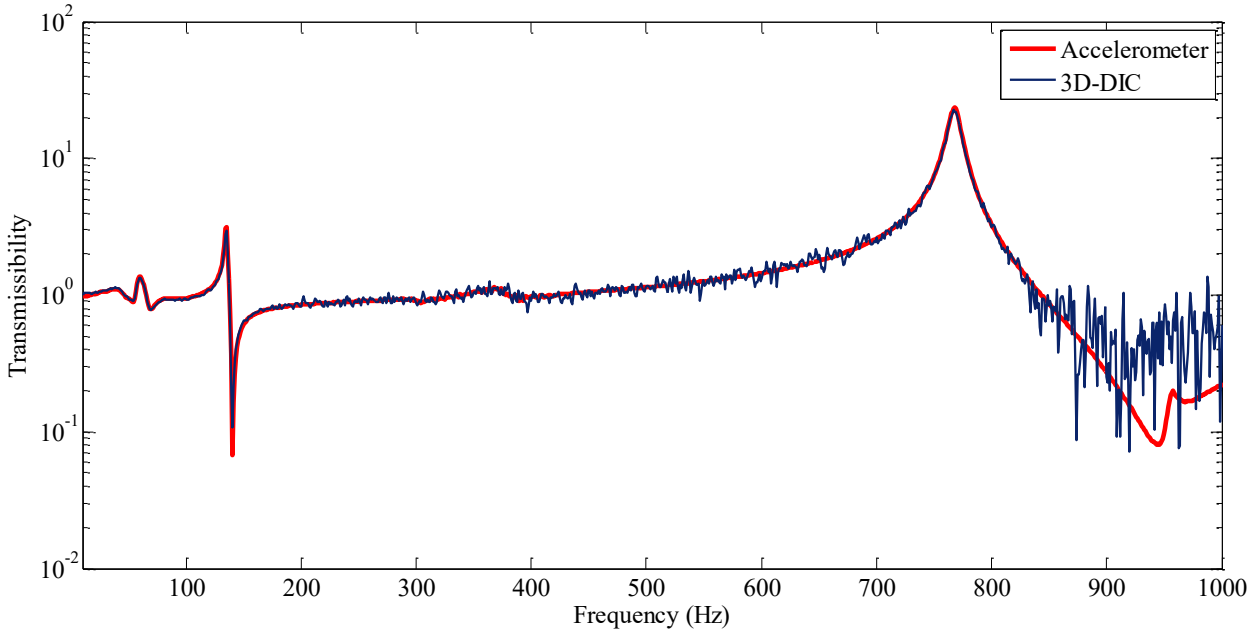

Figure 4: Transmissibility function at the point placed at 35 mm from the clamped edge, where the validation accelerometer was located

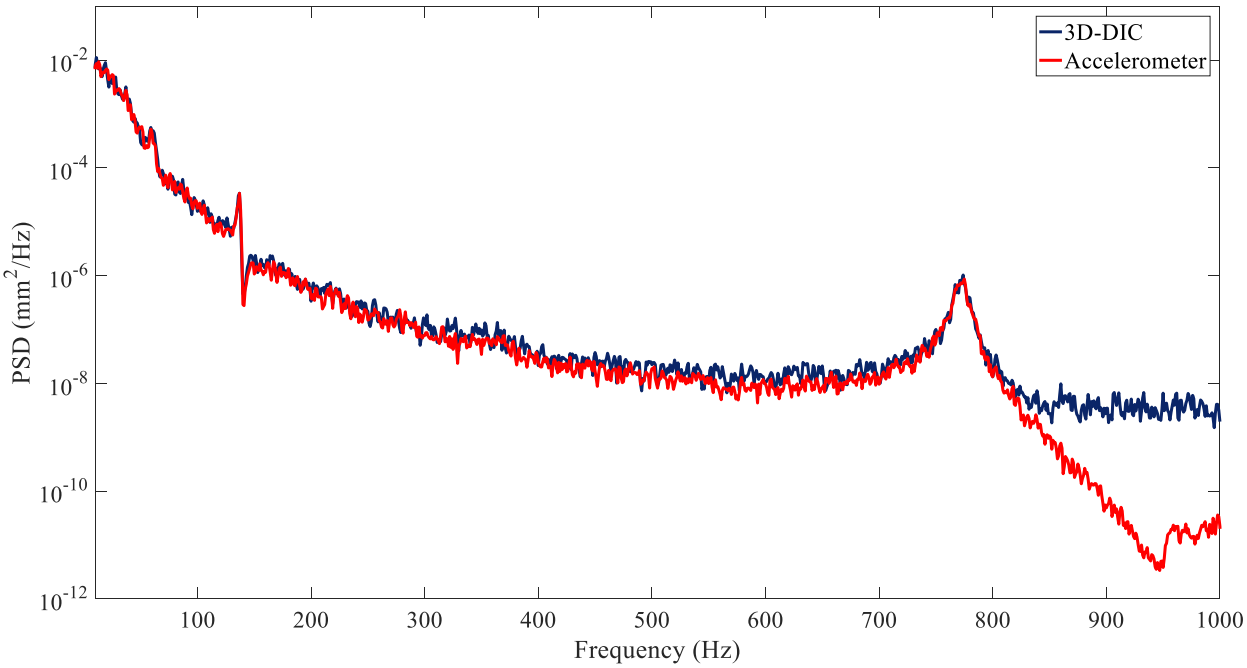

Figure 5: Transmissibility function at the point placed at 35 mm from the clamped edge, where the validation accelerometer was located

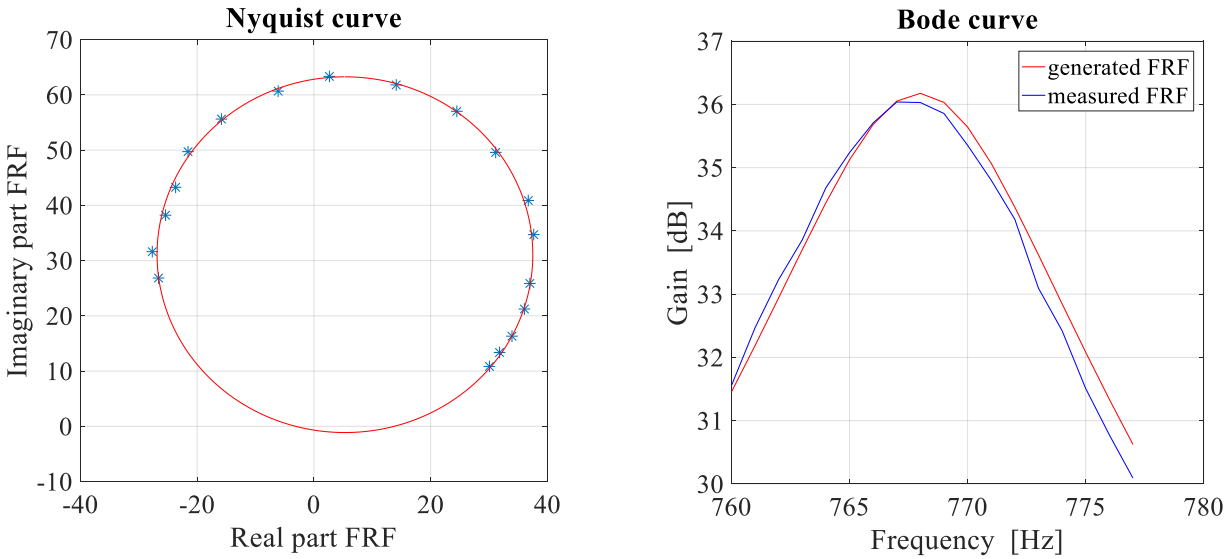

Figure 6: Circle-fitting diagrams of the second mode at a point

Table 2 contains the natural frequencies obtained by means of the three methods here proposed. Although slightly differences can be observed, results seem to be really consistent.

Table 2: Natural frequencies (Hz) of the cantilever beam

Mode	Experimental	FEM	Theoretical
1	135.38	131.03	129.34
2	767.78	817.81	810.41

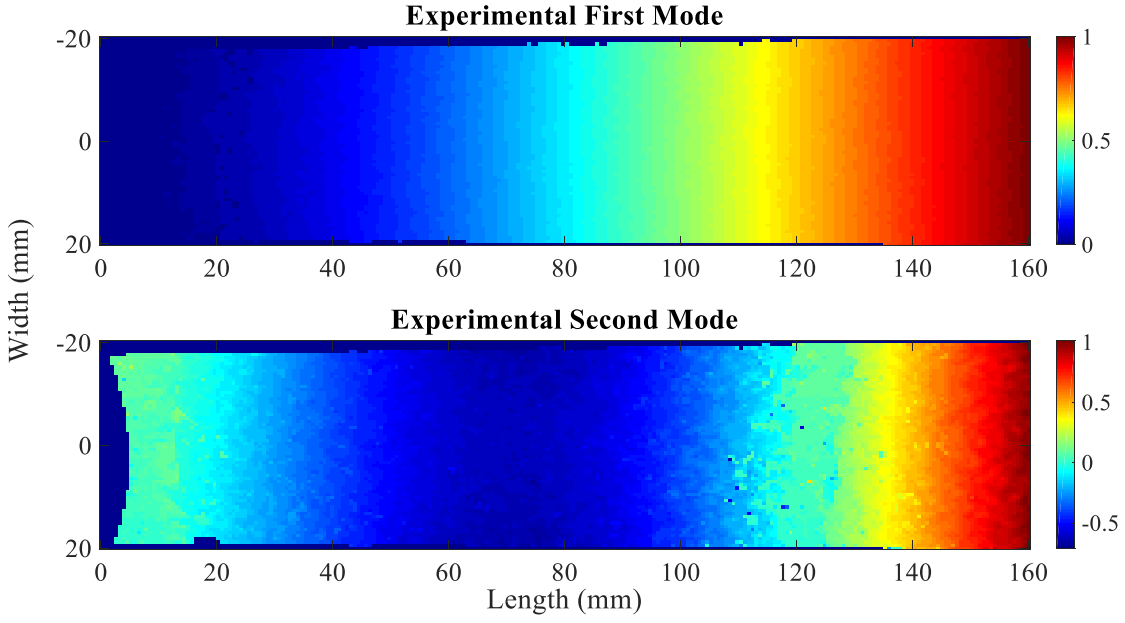

Figure 7: Experimental mode shapes of the first two bending modes using DIC

Experimental mode shape reconstruction consisted in plotting the amplitudes from every single point of the amplitude matrix. This representation is presented in Fig. 7, where both modes can be seen with non-dimensional normalised values. Both modes present maximum displacement at 160 mm, i.e., the released tip and zero-displacement when getting closer to the clamping at 0 mm. The second mode presents another node of zero-displacement, located around 120 mm of length coordi-

nate what is typical of this kind of second bending mode. Thus, results describes the expected behaviour, described by theoretical and FEM models as well. It can be seen that the second mode shape is noisier than the first one. It must be considered that the level of displacement at 767.78 Hz is much lower than at 135.38 Hz, as seen in Fig. 5. Despite that, DIC properly registered it.

Finally, in order to validate the mode shapes obtained experimentally by DIC using the proposed methodology, MAC was applied between experimental mode shapes and those from FEM and theoretical analysis. The results, in Table 3, show that there is a great correspondence, indicated by correlation values close to one.

Table 3: MAC matrices comparing experimental mode shapes with FEM and theoretical modes

		Experimental modal analysis	
		$f_1 = 135.38$ Hz	$f_2 = 767.49$ Hz
FEM analysis	$f_1 = 130.19$ Hz	**1.0000**	0.0175
	$f_2 = 812.60$ Hz	0.0020	**0.9836**
Theoretical analysis	$f_1 = 128.52$ Hz	**0.9999**	0.0167
	$f_2 = 805.25$ Hz	0.0023	**0.9841**

5. Conclusions

In this work are involved some interesting features for full-field modal identification using HS 3D-DIC when base excitation test are required. Circle-fit approach is proposed as a non-demanding method considering the amount of processed data. Transmissibility function, directly obtained from measurements, are transformed into their equivalent FRFs for proper circle-fit method application under single degree of freedom assumptions. As a result, natural frequencies, mode shapes and damping ratios were determined without the support of any other techniques, nor the execution of additional tests. That would be the case of other studies which employed sinusoidal excitation so as to determine mode shapes. This methodology, applied to a cantilever beam, have proved to be consistent and accurate. Great homogeneity was achieve along the beam in natural frequencies and damping ratios full-field estimation. Accuracy was proved by comparing DIC measurement with accelerometer measurement. Furthermore, the methodology was validated by comparing with analytical and numerical models. Experimental natural frequencies were similar with those from these models. In particular, mode shape comparison was quantitatively made by means of MAC indicator, which showed good correlation.

REFERENCES

1 Ewins, D. J., *Modal Testing: Theory, Practice, and Application*, 2nd ed. Research Studies Press Ltd (2000).

2 Schreier, H., Orteu, J.-J., and Sutton, M. A., *Image Correlation for Shape, Motion and Deformation Measurements*. Springer US, Boston, MA (2009).

3 Warren, C., Niezrecki, C., Avitabile, P., and Pingle, P. Comparison of FRF measurements and mode shapes determined using optically image based, laser, and accelerometer measurements, *Mechanical Systems and Signal Processing*, **25** (6), 2191–2202, (2011).

4 Wang, W., Mottershead, J. E., Siebert, T., and Pipino, A. Frequency response functions of shape features from full-field vibration measurements using digital image correlation, *Mechanical Systems and Signal Processing*, **28**, 333–347, (2012).

5 Reu, P. L., Rohe, D. P., and Jacobs, L. D. Comparison of DIC and LDV for practical vibration and modal measurements, *Mechanical Systems and Signal Processing*, **86**, 2–16, (2017).

6 Béliveau, J. G., Vigneron, F. R., Soucy, Y., and Draisey, S. Modal parameter estimation from base excitation, *Journal of Sound and Vibration*, **107**, 435–449, (1986).

7 Ha, N. S., Vang, H. M., and Goo, N. S. Modal Analysis Using Digital Image Correlation Technique: An Application to Artificial Wing Mimicking Beetle's Hind Wing, *Experimental Mechanics*, 989–998, (2015).

8 Validation of Numerical Engineering Simulations: Standardisation Actions (VANESSA). European FP7 project grant agreement no. NMP3-SA-2012-319116, 2014. [Online]. Available: http://www.engineeringvalidation.org/. [Accessed: 31-May-2016].

9 Kouroussis, G., Fekih, L. Ben, Conti, C., and Verlinden, O.Easymod : a Matlab / Scilab Toolbox for Teach- Ing Modal Analysis, in *Proceedings of the 19th International Congress on Sound and Vibration*, (2012).

10 Allemang, R. J. and Brown, D. L. A correlation coefficient for modal vector analysis, *First International Modal Analysis Conference*, 110–116, (1982).

11 Blevins, R. D., *Formulas for natural frequency and mode shape*. Krieger Publishing Company (2001).